

# Reactor System Analysis and Pellet Injection Simulation in Helical and Tokamak Reactors

Y. Higashiyama, K. Yamazaki, J. Garcia<sup>a</sup>, H. Arimoto, T. Shoji

*Nagoya University, Furo-cho, Chikusaku, Nagoya 464-8603, Japan*

*<sup>a</sup>Universitat Politècnica de Catalunya (UPC), Barcelona, Spain*

In the future fusion reactor, the plasma density peaking is important for the increase in the fusion power gain and for the achievement of confinement improvement mode. The density control and the internal transport barrier (ITB) formation due to the pellet injection has been simulated in tokamak and helical reactors using the toroidal transport linkage code TOTAL. Firstly, the pellet injection simulation is carried out including the neutral gas shielding model and the mass relocation model in the TOTAL code, and the effectiveness of the high field side (HFS) pellet injection is clarified. Secondly, the ITB simulation with the pellet injection is carried out with the confinement improvement model based on the ExB shear effects, and it is found that the deep pellet penetration is helpful for the ITB formation as well as the plasma core fuelling in the reversed shear tokamak reactor, but the deep pellet penetration is not effective in the helical reactor.

Keywords: Transport simulation, Internal transport barrier, Pellet injection, Tokamak reactor, Helical reactor

## 1. Introduction

The total fusion reactor power strongly depends on the radial profile of plasma temperature and density, and the density control is important to optimize reactor operation. To control plasma density and pressure profiles, the pellet injection is considered as a prospective technique. The pellet injection is used for the plasma core fuelling, and it brings a peaked density profile, so that the fusion power gain is increased. In JET and other tokamak experiments, it was shown that the density profile modifications disagree with pellet ablation theory [1] that assumes the pellet particles remain on the magnetic field lines where they are ionized [2]. The pellet penetration depth measured by the pellet light emission agreed well with the pellet ablation theory. This suggested that a fast outward major-radius drift may occur during the pellet ablation and toroidal symmetrization processes. To test this hypothesis the experiment of the high-field side (HFS) pellet injection has done in ASDEX-Upgrade, and it was shown that the fuelling efficiency and the penetration depth of pellets are improved [3]. The similar results are observed in DIII-D [4] and other tokamak experiments, and the HFS pellet injection is expected to be an effective technique of plasma core fuelling in future tokamak reactors.

The transport simulation studies have been carried out focusing on the ITB formation in tokamak and helical plasmas. When the ITB is formed in the plasma, it brings good confinement and rather peaked pressure profile, so

that the operation scenarios with the ITB in tokamaks are expected as enhanced performance modes such as high  $\beta_p$  mode [5], reversed shear mode [6], and pellet enhanced performance mode (PEP) [7,8]. In helical systems the ITB model based on Bohm and GyroBohm-like transport with ExB shear flow effects has already been compared with the LHD experimental ITB [9] and this model is inspired from the JET mixed-model [10]. This model is introduced into the toroidal transport linkage TOTAL code [11, 12], and is applied to the 1-dimensional (1-D) ITB formation simulation of both 3-D equilibrium helical and 2-D equilibrium tokamak plasmas.

Both the pellet injection and the ITB formation have big influence on the density profile and the fusion power output, so that we consider about operation scenario with ITB formation by pellet injection density control in helical and tokamak reactor plasmas by using the TOTAL code. Section 2 will describe the details of the transport models and the HFS pellet injection model included in the TOTAL code, and simulation results will be shown in section 3. The conclusion will be given in section 4.

## 2. TOTAL code

### 2.1. Transport model description

The Bohm and GyroBohm mixed transport model with the ExB shear flow effect has already been compared with the helical and tokamak experimental ITBs [9, 10]. The most widely accepted explanation for the ITB formation relies on the suppression of ITG

turbulence due to ExB shear flow. The suppression of the turbulence might occur when the ExB flow shearing rate  $\omega_{ExB}$  exceeds the ITG linear growth rate  $\gamma_{ITG}$ . The shearing rate  $\omega_{ExB}$  is defined as [13,14]

$$\omega_{ExB} = \left( \frac{\Delta\psi_0}{\Delta\phi_0} \right) \frac{\partial^2 \Phi_0(\psi)}{\partial \psi^2} \cong \left| \frac{RB_\theta}{B_\phi} \frac{\partial}{\partial r} \left( \frac{E_r}{RB_\theta} \right) \right|, \quad (1)$$

where  $\Delta\psi_0$  and  $\Delta\phi_0$  are the correlation lengths of the ambient turbulence in the radial and toroidal direction, and  $\Phi_0$ ,  $E_r$ ,  $B_\theta$  and  $B_\phi$  are the equilibrium electrostatic potential, the radial electric field, the poloidal and toroidal magnetic field, respectively. In tokamaks, the radial electric field  $E_r$  is not easily measured directly, so that  $E_r$  can be calculated from the plasma radial force balance equation under the assumption that the poloidal velocities can be expressed according to the neoclassical theory [15, 16]. However in this paper,  $E_r$  is described simply as

$$\frac{dE_r}{dr} \cong -\frac{1}{en_i^2} \frac{dn_i}{dr} \frac{dp_i}{dr}, \quad (2)$$

in the H-mode condition [17], where  $n_i$  and  $p_i$  are ion density and ion pressure, respectively. The ITG growth rate  $\gamma_{ITG}$  is defined as [18]

$$\gamma_{ITG} = \frac{(\eta_i - 2/3)^{1/2} |s| c_i}{qR}, \quad (3)$$

where  $\eta_i = L_n/L_T$ ,  $c_i = \sqrt{T_i/m_i}$ , and  $s$  is the magnetic shear defined as

$$s = \frac{r}{q} \left( \frac{dq}{dr} \right). \quad (4)$$

Most theoretical studies based on the ExB shear stabilization adopt a thermal diffusion coefficient  $\chi$  in the form

$$\chi_{e,i} = \chi_{neoclassical} + \chi_{anomalous}, \quad (5)$$

$$\chi_{anomalous} = \alpha_1 \times \chi_{Gyrobohm} + \alpha_2 \times \chi_{Bohm} \times F \left( \frac{\omega_{ExB}}{\gamma_{ITG}} \right), \quad (6)$$

where

$$F \left( \frac{\omega_{ExB}}{\gamma_{ITG}} \right) = \frac{1}{1 + \left( \frac{\omega_{ExB}}{\gamma_{ITG}} \right)^2}. \quad (7)$$

The coefficient  $\chi_{neoclassical}$  is the neoclassical part of thermal diffusion coefficient, and  $\chi_{anomalous}$  is the anomalous part described as the Bohm and GyroBohm mixed transport model [9, 10]. And particle diffusion coefficient  $D$  is assumed as  $D = \chi_{e,i} / C_{ano}$ , in this paper  $C_{ano} = 3$  (tokamak) and 1 (helical).

## 2.2. HFS pellet injection

The high-field-side (HFS) pellet injection is described as two processes which are the pellet ablation and the mass relocation. We simulate the HFS injection with the pellet penetration model combined with the ablation model and the mass relocation model. There are a few models which satisfactorily describe the pellet ablation and give similar results [19]. So, we use here the most popular one: the neutral gas shielding (NGS) model [1]. The mass relocation width from ablation point with the plasmoid drift in the major-radius direction  $\Delta R$  is described as [20]

$$\Delta R = -0.5q\beta B_i B_p^{-1} (1 + qL_e/a)^{-1} \times a^{-2} r_0^2 \delta n (n + \langle \delta n \rangle)^{-1}. \quad (8)$$

## 3. Simulation results

### 3.1. Demonstration of HFS pellet injection

The reactor machine parameters used in this paper were those of typical designs optimized using the reactor design system code PEC (Physics- Engineering- Cost) [12]. These parameters are derived from two 1GW electric power fusion reactor designs; high-field high-beta compact tokamak reactor TR-1 (major radius  $R=5.2m$ , magnetic field  $B=7.1T$ ) and high-beta helical system HR-1 ( $R=12.1m$ ,  $B=4.6T$ ).

Typical results of the HFS pellet injection simulation in tokamak reactor are shown in figure 1. The pellet ablation densities are shown for the different pellet injection velocity. Here, the radial parabolic temperature and flat density profiles are assumed as  $T(x) = T_0(1-x^2)^3$ ,  $n(x) = n_0(1-x^2)^{0.5}$  with  $T_0 = 30keV$  and  $\langle n \rangle = 10^{20}m^{-3}$ . This figure shows that the HFS injection could provide rather deep fuelling in the reactor-grade tokamak plasma, and the further increase in the injection velocity improves the central fuelling. For assumed temperature and density

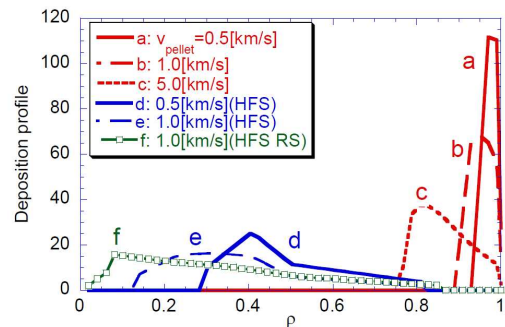


**Figure 1.** Model prediction for the HFS pellet injection in tokamak reactor. Ablation profiles are shown by a, b and c, and HFS injection simulation results are given by d, e, and f depending on the pellet injection velocities. The profiles d and e are in the normal shear case, and f is in the reversed shear case.

profiles, the HFS injection with the pellet velocity of 1 km/s could provide the density increase at the normalized radius  $r/a \sim 0.1$ . Moreover, it shows that the reversed shear mode improves the central fuelling for the HFS injection based on the mass relocation model of equation (8).

### 3.2. ITB simulation with pellet injection

In the previous subsection, we show that the pellet injection could provide deep fuelling in tokamak reactor by the HFS injection. So that we consider about operation scenario with ITB formation in deep (by HFS injection) and shallow (by medium field side injection) penetration depth cases in the reversed shear ITB plasmas.

The figure 2 shows the operation scenarios of the tokamak reactor (reversed shear mode) in deep penetration case by HFS pellet injection. Alpha particle power and density are feedback-controlled by the adjustment of both heating power and fuelling. In this scenario, ITB is formed at 15 sec and plasma is ignited at 100 sec. The figure 3 shows the comparisons with radial profiles at steady state (time=200 sec) in deep (same as figure 2) and shallow cases. We can see that there are clear differences between both cases. In the deep penetration case shown in the left-hand of the figure 3, the ITB is formed at  $\rho \sim 0.4$ , but in the shallow case in the right-hand figure the ITB is not formed.

This reason is shown in the bottom two figures in figure 3. In this simulation, the ITB formation is determined by two parameters,  $\omega_{ExB}$  and  $\gamma_{ITG}$ . In both cases,  $\gamma_{ITG}$  is reduced at  $\rho \sim 0.4$  where the magnetic shear  $s \sim 0$ . The suppression occurs when  $\omega_{ExB}$  exceeds  $\gamma_{ITG}$ , so the ITB tends to be formed at low  $\gamma_{ITG}$  position. However,

in the shallow penetration case the rate  $\omega_{ExB}$  is small at  $\rho \sim 0.4$ , because the gradient of radial electric field  $dE_r/dr$  is small depending on the term  $dn_i/dr$  in equation (2). The transient density profile and the relevant clear ITB formation depend on the pellet penetration depth. The deeper pellet penetration brings the larger gradient of  $E_r$  and the larger shearing rate  $\omega_{ExB}$  at the position of small  $\gamma_{ITG}$ , so that the ITB is formed there. We can say that the deep pellet penetration plays an important role in the ITB formation, and the HFS pellet injection is a quite effective technique for the confinement improvement as well as the core density fuelling in the reversed shear tokamak reactor.

Figure 4 shows the results of the ITB simulation in the helical reactor. It is compared with deep and shallow pellet penetration depth cases (same in tokamak). In this simulation, different from tokamak case, the deep penetration case corresponds to the high speed pellet injection and not to the HFS injection, because the effectiveness of HFS injection has not been observed so far in helical system [21]. This might be because the field connection length between the high field side and the low field side is quite short in comparison with tokamak case. In the helical reactor, the radial electric field is determined from the ambipolarity condition of helical ripple-induced neoclassical flux, and the large gradient of radial electric field appears at the position of pellet penetration ‘toe point’ (after this, we call this large electric field gradient the ‘sharp valley’). The electric field is influenced by the pellet penetration depth through

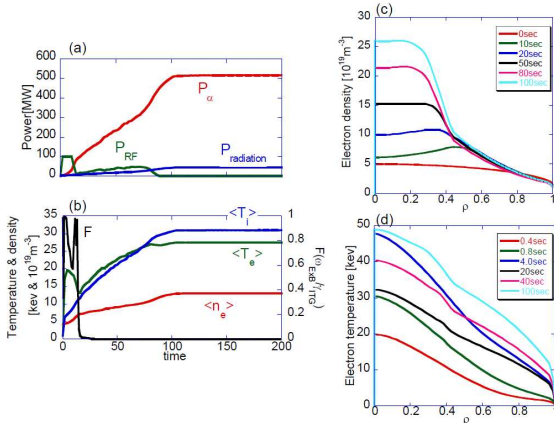


**Figure 2.** Figure (a) and (b) show the operation scenarios of the TR-1 (reversed shear) with HFS pellet injection. The improvement factor  $F(\omega_{ExB}/\gamma_{ITG})$  which is defined in the equation (7) is the value at  $\rho=0.4$ . Figure (c) and (d) show the time evolution of the electron density and temperature radial profiles.

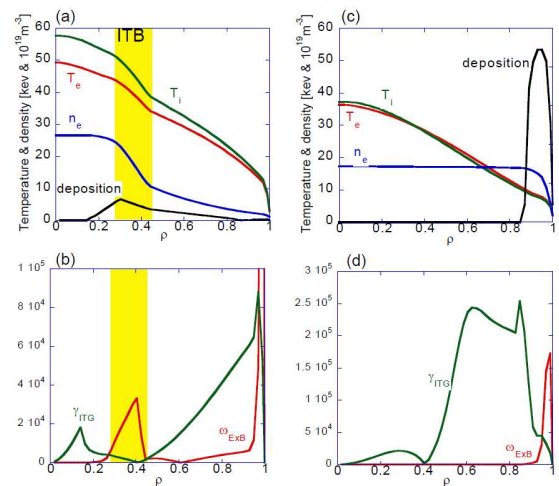


**Figure 3.** ITB simulation results with pellet injection in the reversed shear tokamak reactor. Left figures denote deep pellet penetration case (by HFS), and right figures are shallow penetration case (by the medium field side injection). The upper figures (a) and (c) show ion and electron temperatures, electron density, and pellet deposition profiles, and the lower figures (b) and (d) show  $\omega_{ExB}$  and  $\gamma_{ITG}$  profiles.

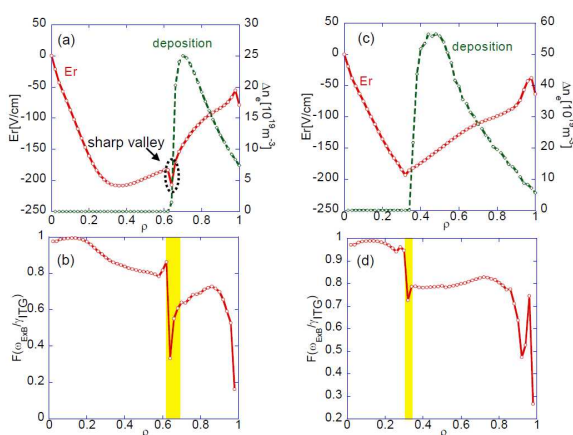


**Figure 4.** ITB simulation results with pellet injection in helical reactor. The left-hand figure corresponds to the shallow penetration case (pellet size = 4mm, injection velocity = 1.0 km/s), and the right-hand figure is the deep penetration case (pellet size = 6mm, injection velocity = 5.0 km/s). The upper figures (a),(c) show radial electric field and pellet deposition profiles, and the lower figures (b),(d) shows the improvement factor  $F(\omega_{ExB}/\gamma_{ITG})$  which is defined in the equation (7).

the density profile, which is similar to the tokamak case. But it is not same as in the tokamak that the ITB is formed in the both deep and shallow cases. The ‘sharp valley’ can be formed at the ‘toe point’ of the pellet penetration as shown in figure 4. In the deeper penetration case the sharp valley tends to be smaller, and the shearing rate  $\omega_{ExB}$  becomes smaller, therefore the reduction in the anomalous transport becomes weaker. These results show that the deeper pellet penetration is not needed for the ITB formation in the helical reactor.

#### 4. Conclusion

We investigated the relationship between the ITB formation and the pellet injection in tokamak and helical reactors. The high field side (HFS) pellet injection in the tokamak reactor was analyzed and its effectiveness was clarified. In the tokamak reactor with reversed shear profile, it was shown that the pellet penetration depth plays an important role in the ITB formation, and the HFS injection would be an effective technique for the confinement improvement as well as the plasma core fuelling. In the helical reactor, we showed that the deep pellet penetration is not needed for the ITB formation because the position of ITB is determined by the ambipolar radial electric field ‘sharp valley’ and the pellet penetration ‘toe point’, and the deeper penetration does not help the strong reduction in anomalous plasma transport.

#### References

- [1] Parks P B and Turnbull R J 1978 *Phys. Fluids* **21** 1735
- [2] Baylor L R *et al* 1992 *Nucl. Fusion* **32** 2177
- [3] Lang P T *et al* 1997 *Phys. Rev. Lett.* **79** 1478
- [4] Baylor L R *et al* 1998 *Fusion Technol.* **34** 425
- [5] Ishida S *et al* 1993 *Proc. 14th Int. Conf. Plasma Physics Controlled Nuclear Fusion Research (Wurzburg,1992)* vol 1 (Vienna: IAEA) p 219
- [6] Kimura H *et al* 1996 *Phys. Plasmas* **3** 1943
- [7] JET Team (presented by Schmidt G L) 1989 *Proc. 12th Int. Conf. Plasma Physics and Controlled Nuclear Fusion Research (Nice, 1988)* vol 1 (Vienna: IAEA) p 215
- [8] Tubbing B *et al* 1991 *Nucl. Fusion* **31** 839
- [9] Garcia J, Yamazaki K, Dies J and Izquierdo J 2006 *Phys. Rev. Lett.* **96** 105007
- [10] Tala T *et al* 2001 *Plasma Phys. Control. Fusion* **43** 507
- [11] Yamazaki K and Amano T 1992 *Nucl. Fusion* **32** 633.
- [12] Yamazaki K *et al* 2006 *Fusion Engineering and Design* **81** 2743
- [13] Hahn T S and Burrell K H 1995 *Phys. Plasmas* **2** 1648
- [14] Zhou P, Horton W and Sugama H 1999 *Phys. Plasmas* **6** 2503
- [15] Ernst D R *et al* 2000 *Phys. Plasmas* **7**, 615
- [16] Kim Y B, Diamond P H and Groebner R J 1991 *Phys. Fluids B* **3** 2050
- [17] Hinton F L and Staebler G M 1993 *Phys. Fluids B* **5** 1281
- [18] Esposito B *et al* 2003 *Plasma Phys. Control. Fusion* **45** 933
- [19] Baylor L R *et al* 1997 *Nucl. Fusion* **37** 445
- [20] Polevoi A R and Shimada M 2001 *Plasma Phys. Control. Fusion* **43** 1525
- [21] Sakamoto R *et al* 2002 *Plasma Phys. Control. Fusion* **26B**, P-1.074